ACADEMIC PRESS

Available online at www.sciencedirect.com

SCIENCE DIRECT®

Cellular Immunology 220 (2002) 107–115

Cellular Immunology

www.elsevier.com/locate/ycimm

Rapid changes in shape and number of MHC class II expressing cells in rat airways after *Mycoplasma pulmonis* infection

Eric Y. Umemoto,[a,1] James J. Brokaw,[b,*] Marc Dupuis,[a,2] and Donald M. McDonald[a]

[a] *Cardiovascular Research Institute, Department of Anatomy, and Comprehensive Cancer Center, University of California, San Francisco, CA 94143, USA*

[b] *Office of Medical Student Affairs, Department of Anatomy and Cell Biology, Indiana University School of Medicine, Medical Science Building, Room 164, 635 Barnhill Drive, Indianapolis, IN 46202-5120, USA*

Received 28 June 2002; accepted 6 January 2003

Abstract

Mycoplasma pulmonis infection in rodents causes a chronic inflammatory airway disease with a strong immunological component, leading to mucosal remodeling and angiogenesis. We sought to determine the effect of this infection on the shape and number of dendritic cells and other major histocompatibility complex (MHC) class II expressing cells in the airway mucosa of Wistar rats. Changes in the shape of subepithelial OX6 (anti-MHC class II)-immunoreactive cells were evident in the tracheal mucosa 2 days after intranasal inoculation with *M. pulmonis*. By 1 week, the shape of the cells had changed from stellate to rounded (mean shape index increased from 0.42 to 0.77). The number of OX6-positive cells was increased 6-fold at 1 week and 16-fold at 4 weeks. Coincident with these changes, many columnar epithelial cells developed OX6 immunoreactivity, which was still present at 4 weeks. We conclude that *M. pulmonis* infection creates a potent immunologic stimulus that augments and transforms the OX6-immunoreactive cell population in the airways by changing the functional state of airway dendritic cells, initiating an influx of MHC class II expressing cells, and activating expression of MHC class II molecules by airway epithelial cells.

Keywords: Antigen-presenting cells; Chronic inflammation; Dendritic cells; Immunohistochemistry; Morphometry; OX6; Trachea

1. Introduction

Antigen presentation by cells expressing major histocompatibility complex class II (MHC class II) molecules on their surface is an important step in the initiation of the primary immune response [1]. Dendritic cells (DC) are the principal MHC class II expressing cells in the normal airway mucosa. These cells play a major role in the processing of inhaled antigens and may participate in the pathogenesis of infectious and allergic airway diseases [2–4]. During steady-state conditions, DC turnover every 36–48 h [5]. However, the DC network rapidly expands after exposure to a variety of pathogens and antigens [6]. For example, exposure to aerosolized heat-inactivated *Moraxella catarrhalis* causes DC influx into the airways which peaks within 3 h and remains elevated for 48 h [5]. Inoculation of viable *Bordatella pertussis* results in DC recruitment with similar kinetics but with a maximal cell density at 24 h [7]. Even at the peak of the inflammatory response, DC are the principal MHC class II expressing cells—greatly outnumbering macrophages and B lymphocytes [7]. Such stimuli can also evoke transient expression of MHC class II molecules by airway epithelial cells [8–10].

Less is known about the involvement of DC and other MHC class II expressing cells in chronic inflammatory airway disease, in part because most disease models have focused on transient conditions. The long-lasting consequences of *Mycoplasma pulmonis* infection make it useful for studying changes in chronic disease

* Corresponding author. Fax: +317-274-4309.
E-mail address: jbrokaw@iupui.edu (J.J. Brokaw).
[1] Present address: Department of Microbiology, University of Hawaii, 2538 The Mall, Snyder Hall 207, Honolulu, HI 96822, USA.
[2] Present address: NovImmune SA, Fondation pour Recherches Médicales, 64 avenue de la Roseraie, 1205 Genève, Switzerland.

0008-8749/03/$ - see front matter © 2003 Published by Elsevier Science (USA).
doi:10.1016/S0008-8749(03)00026-1

[11–13]. The organisms attach to the luminal surface of the airway epithelium of rats and mice [12] and are not cleared from the airways despite strong cellular and humoral immune responses [11,13–15]. The ongoing stimulus causes an influx of mononuclear cells, including DC, macrophages, and lymphocytes [15–18]. The development of mucosal lymphoid tissue is a prominent part of the remodeling of the airway mucosa, and is accompanied by epithelial cell and mucous gland hyperplasia, fibrosis, angiogenesis, and increased sensitivity of the newly formed blood vessels to the neuropeptide substance P [13,14,19,20]. Although some of these changes may occur after viral infection [20,21], *M. pulmonis* infection is unusual in that it causes life-long disease and, if untreated, can result in severe remodeling of the airway mucosa [22]. The role of DC and other MHC class II expressing cells in these changes is unknown [16,17], but is of interest because of the rapid cellular response after infection and the strong immunological component of mycoplasmal airway disease.

In the present study, we used *M. pulmonis* infection as a model of chronic inflammation to determine the time course of changes in shape, number, and distribution of MHC class II expressing cells in the airway mucosa, with a focus on the region beneath the airway epithelium where *M. pulmonis* organisms are attached. We also determined whether epithelial cells express MHC class II molecules after *M. pulmonis* infection.

MHC class II expressing cells in the tracheal mucosa, stained immunohistochemically with the OX6 monoclonal antibody [3,4,23], were examined in rats infected with *M. pulmonis* for 2 days to 4 weeks. Tracheal whole mounts were used to determine the 3-dimensional shape and number of OX6-immunoreactive cells within and near the airway epithelium, and tracheal cross-sections were used to determine the distribution of these cells within the thickness of the airway wall.

2. Materials and methods

2.1. Animals

Male pathogen-free Wistar rats were purchased from Charles River Breeding Laboratories (Hollister, CA) and housed under barrier conditions in autoclaved microisolator units, three animals per cage. Charles River documented the pathogen-free status of the animals as evidenced by serological assays for multiple pathogens, including *M. pulmonis*, parainfluenza type I (Sendai) virus, coronavirus (rat coronavirus/sialodacryoadenitis virus), and cilia-associated respiratory bacillus. Animals were 7 weeks old and 175–200 g upon arrival. All experiments were approved by the Committee on Animal Research at the University of California, San Francisco.

2.2. M. pulmonis infection

M. pulmonis strain 5782C was grown in mycoplasma broth, harvested in the late log phase of growth, and frozen at −70 °C in 1 ml aliquots [24,25]. The frozen aliquots contained 7.5×10^9 colony forming units of *M. pulmonis* per milliliter, as determined by quantitative culture [24,25]. After anesthesia (intramuscular injection of 0.11–0.15 ml of a mixture of ketamine, 83.3 mg/ml, Parke-Davis, Morris Plains, NJ, and xylazine, 3.3 mg/ml, The Butler, Columbus, OH), rats were inoculated intranasally with 100 µl aliquots of *M. pulmonis* medium or sterile culture medium into each nostril daily, on three consecutive days [13].

2.3. Experimental protocol

At 2 or 4 days or 1, 2, or 4 weeks after the first inoculation, rats ($n = 5$ per time-point) were anesthetized by intraperitoneal injection of sodium pentobarbital (50 mg/kg, Abbott Laboratories, North Chicago, IL) and then perfused via the ascending aorta for 2 min with 1% paraformaldehyde in phosphate-buffered 0.9% NaCl (PBS, pH 7.4) at 120–140 mmHg. Pathogen-free controls included five uninoculated rats and six rats inoculated with sterile culture medium (three rats at 2 days and three rats at 1 week). All animals had 1 ml of blood drawn from an external jugular vein for measurement of serological antibody titers to *M. pulmonis*, Sendai virus, and rat coronavirus/sialodacryoadenitis virus. After the vascular perfusion of fixative, tracheas were removed and fixed in 4% paraformaldehyde for 1–7 days at 4 °C before being processing for immunohistochemistry.

2.4. Immunohistochemistry

Tracheas, washed and permeabilized in six 1-h changes of PBS containing 0.3% Triton X-100 (PBS/Triton at room temperature, Sigma), were cut transversely into three segments, then were incised longitudinally and pinned flat, mucosal surface up, on Sylgard slabs (Dow Corning, Midland, MI). Alternatively, 150-µm cross-sections were cut with a Vibratome (Series 1000, Technical Products International, St. Louis, MO).

Tracheal whole mounts or cross-sections were processed for immunoperoxidase histochemistry using techniques described previously [26,27]. Briefly, specimens were incubated for 2 h in PBS containing 5% normal goat serum (Jackson ImmunoResearch Laboratories, West Grove, PA) and then for 36 h in PBS containing 1% normal goat serum and MRC OX6 anti-MHC class II monoclonal antibody (PharMingen, San Diego, CA) at a 1:1000 dilution [3,4]. The tissues were washed again for 6 h in PBS followed by a 24-h incubation in peroxidase-conjugated goat anti-mouse IgG

(Jackson) at a 1:200 dilution. The solutions contained 0.01% thimerosal (Sigma) to prevent microbial growth. Another wash in PBS was followed by 10 min in 0.05 M Trizma base–Trizma HCl buffer (Sigma), pH 7.6, containing 0.05% diaminobenzidine and 0.01% hydrogen peroxide to localize the peroxidase-labeled secondary antibody. All steps were done at room temperature. Finally, the specimens were dehydrated in ethanol, cleared in toluene, and mounted in Permount (Fisher Scientific, Fair Lawn, NJ). Whole mounts were mounted mucosal surface up.

Tracheas were examined with a Zeiss Axiophot microscope (Carl Zeiss, Thornwood, NY) equipped with differential interference contrast optics or with an Edge R400 microscope (Edge Scientific Instrument, Los Angeles, CA), which uses oblique specimen illumination to produce 3-dimensional images. Color photographs taken with Kodak Ektachrome 100 film were scanned (Polaroid SprintScan 35, Cambridge, MA) and printed on a digital image printer (Fujix Pictography 3000, Fuji Film, Tokyo, Japan).

2.5. Shape of OX6-immunoreactive cells

The shape of OX6-immunoreactive (OX6-positive) cells was estimated using a shape-sensitive parameter (shape index $= 4\pi A/P^2$, where A is the projected cell area and P the projected perimeter) that expresses the ratio of area to perimeter relative to that of a circle [28]. Circular cells have a shape index of 1, whereas irregularly shaped cells have smaller shape indices, which decrease toward zero as the perimeter increases with respect to the area. DC with many processes have smaller shape indices than more rounded cells. The projected area and perimeter of 25 OX6-positive cells were measured in the rostral third of each trachea. Measurements were made with a digitizing tablet on real-time color video images magnified with a Zeiss Axiophot microscope (projected magnification approximately 1800×) [28].

2.6. Number of OX6-immunoreactive cells

OX6-positive cells, located within or beneath the epithelium to a depth of about 50 μm, were counted in 12 consecutive regions of mucosa, each measuring 0.09 mm^2, in tracheal whole mounts. These particular cells were selected so the measurements would reflect the cells near the *M. pulmonis* organisms in the airway lumen, and the values would be comparable to published data on subepithelial DC [2,3]. Measurements were made on regions of mucosa over cartilage rings 3–14. The number of OX6-positive cells was expressed per square millimeter of mucosal surface. Specimens were viewed at a projected magnification of 400×. Epithelial basal cells, which had faint immunoreactivity, and columnar epithelial cells, which had variable immunoreactivity after *M. pulmonis* infection, were readily identified and excluded from the counts of DC. Mucosal thickness was measured in tracheal cross-sections.

2.7. Serological titers to pathogens

Serological antibody titers to *M. pulmonis*, Sendai virus, and rat coronavirus/sialodacryoadenitis virus were measured by enzyme-linked immunosorbent assays (ELISA; BioReliance, Rockville, MD).

2.8. Statistical analysis

Values are expressed as means ± SE ($n = 5$ rats per group, unless specified otherwise). The significance of differences between groups was evaluated by analysis of variance and Fisher's test or Scheffé's F test for multiple comparisons or, for values that were not normally distributed, by the Mann–Whitney test. Differences were considered significant when $P < 0.05$.

3. Results

In pathogen-free rats, a network of MHC class II expressing cells, identified by their OX6 immunoreactivity, occupied a thin layer just beneath the epithelium of the tracheal mucosa (Fig. 1A). In rats infected with *M. pulmonis*, the mucosa became progressively thicker and much more densely populated with OX6-positive cells over the 4-week period of the study (Figs. 1B and C). Mucosal thickness increased from about 50 μm in pathogen-free rats to 200 μm at 1 week after infection, and 500 μm at 4 weeks after infection.

3.1. Shape of OX6-immunoreactive cells

Most of the OX6-positive cells in the tracheas of pathogen-free rats had the characteristic branched morphology of DC [3,4,27]. Cells with 3–5 branched cytoplasmic processes formed a thin network roughly in the plane of epithelial basal cells (Fig. 1D). Consistent with their stellate shape, OX6-positive DC in pathogen-free rats had a comparatively low shape index (mean = 0.42; Fig. 2).

After *M. pulmonis* infection, the shape, number, and distribution of OX6-positive cells in the tracheal mucosa underwent conspicuous changes. OX6-positive cells became progressively rounder during the first week (Fig. 1E), as reflected by an increase in shape index from 0.42 in pathogen-free rats to 0.66 at 2 days after infection and to 0.77 at 1 week (Fig. 2). At 2 and 4 days, the shape of many of the cells was intermediate between stellate and round. At 1, 2, and 4 weeks, almost all of the OX6-positive cells had a rounded phenotype.

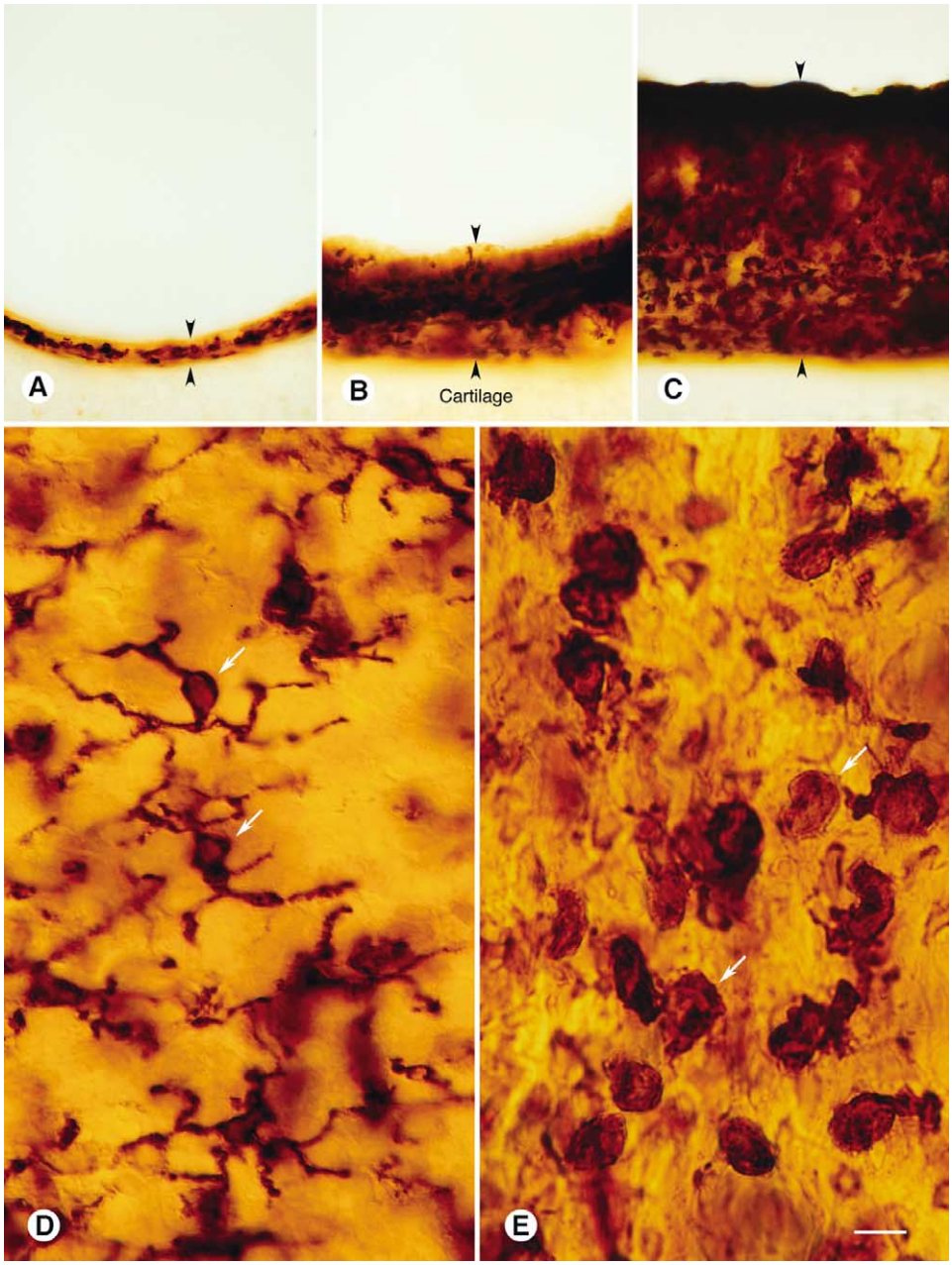

Fig. 1. OX6-immunoreactive cells in rat tracheal mucosa (A–C). Vibratome cross-sections 150 μm in thickness comparing mucosal thickness (arrowheads) and amount of OX6 immunoreactivity in (A) pathogen-free rat, (B) *M. pulmonis*-infected rat at 1 week, and (C) *M. pulmonis*-infected rat at 4 weeks. Cartilage is located beneath the mucosa in all specimens. (D) Tracheal whole mount from pathogen-free rat: OX6-positive cells just beneath epithelium have dendritic shape, with multiple, branched cytoplasmic processes. (E) Tracheal whole mount from rat 1 week after *M. pulmonis* infection: OX6-positive cells near epithelium are rounder and more numerous than corresponding cells in pathogen-free rat. Scale bar in (E) applies to all figures. Bar = 60 μm (A–C), 10 μm (D, E).

OX6 immunoreactivity in tracheas of rats inoculated with sterile culture medium was indistinguishable from that in uninoculated rats. The staining was abolished by omission of the OX6 primary antibody.

3.2. Number of OX6-immunoreactive cells

The numerical density of OX6-positive cells in the most superficial 50 μm of tracheal mucosa increased 58% during the first week after infection, from 1231 ± 89 cells/mm^2 in pathogen-free controls to 1942 ± 101 cells/mm^2 in infected rats ($P < 0.05$; Fig. 3). Increasing OX6 immunoreactivity of mucosal cells made cell-counting more difficult in tracheal whole mounts after the first week; however, an analysis of cross-sections showed that OX6-positive cells were uniformly abundant throughout the mucosa at 1 and 4 weeks after infection (Figs. 1B and C). When mucosal thickening was taken into ac-

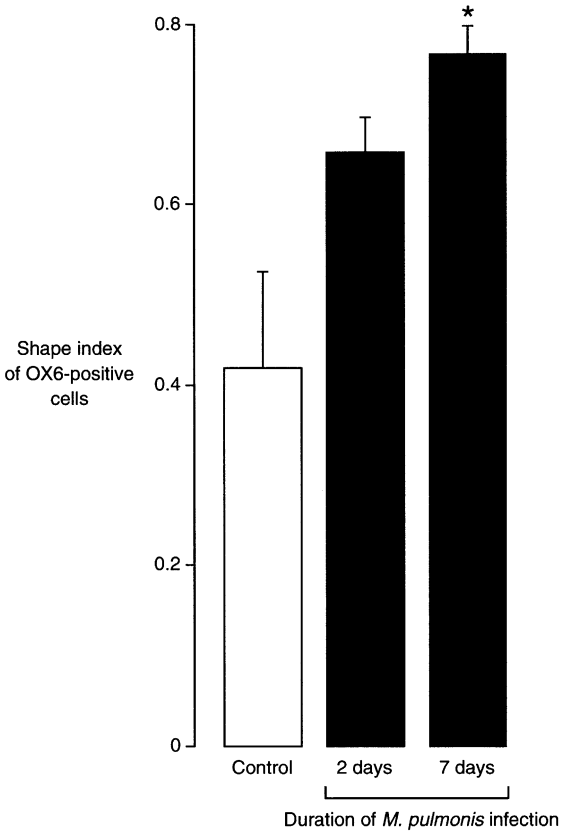

Fig. 2. Shape index of OX6-positive cells. Bar graph showing changes in shape index ($4\pi A/P^2$, where A is the projected cell area and P is the projected cell perimeter) of OX6-positive cells in tracheal whole mounts of pathogen-free rats (control) and rats infected with *M. pulmonis*. Rounder cells have values closer to 1. Values are means ± SE, $n = 5$ rats per group. *Significantly different from control, $P < 0.05$.

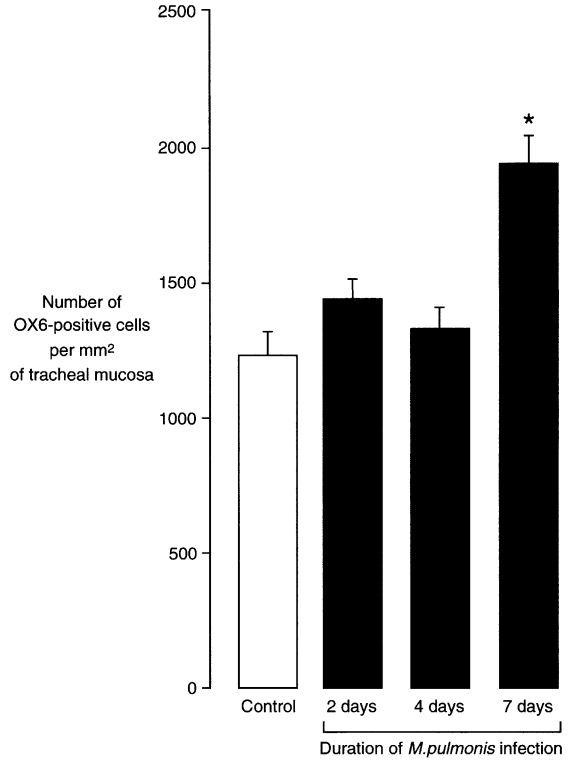

Fig. 3. Number of OX6-positive cells. Bar graph showing number of OX6-positive cells in subepithelial tracheal mucosa of pathogen-free rats (control) and rats infected with *M. pulmonis* ($n = 5$ rats per group). OX6-immunoreactive epithelial cells were not counted. Values are means ± SE of counts made on tracheal whole mounts. *Values significantly different from control, $P < 0.05$.

count, the number of OX6-positive cells was increased 6-fold at 1 week and 16-fold at 4 weeks compared to the pathogen-free value.

3.3. OX6-immunoreactive epithelial cells

In pathogen-free rats, columnar epithelial cells of the tracheal mucosa had no OX6 immunoreactivity, but processes of OX6-positive cells in the lamina propria penetrated the epithelium (Fig. 4A). Some epithelial basal cells had faint immunoreactivity but not a dendritic shape. Scattered columnar epithelial cells had OX6 immunoreactivity at 2 days after infection (Fig. 4B), and the number increased progressively (Fig. 4C). By 1 week, most of the epithelium had granular OX6 immunoreactivity, which appeared to be associated with intracellular organelles (Fig. 4C). No epithelial cells were stained when the OX6 primary antibody was omitted.

3.4. Serological titers to pathogens

Rats that were pathogen-free or infected for 1 week or less did not have significant serological antibody titers to *M. pulmonis*, but at 2 weeks the infected rats had detectable titers (0.14 ± 0.01 ELISA units), and at 4 weeks the titers were significantly higher (0.77 ± 0.07 ELISA units). None of the rats had significant antibody titers to Sendai virus or rat coronavirus/sialodacryoadenitis virus.

4. Discussion

In the present study, *M. pulmonis* infection resulted in conspicuous changes in the shape, number, and distribution of MHC class II expressing cells in the tracheal mucosa. During the first week after infection, OX6-positive cells changed in shape from dendritic to rounded, increased in number, and changed in distribution from a concentration at the base of the epithelium to scattered throughout the mucosa. By 4 weeks, the mucosa had 10 times the normal thickness and an even larger increase in number of OX6-positive cells. In addition, many columnar epithelial cells acquired OX6 immunoreactivity.

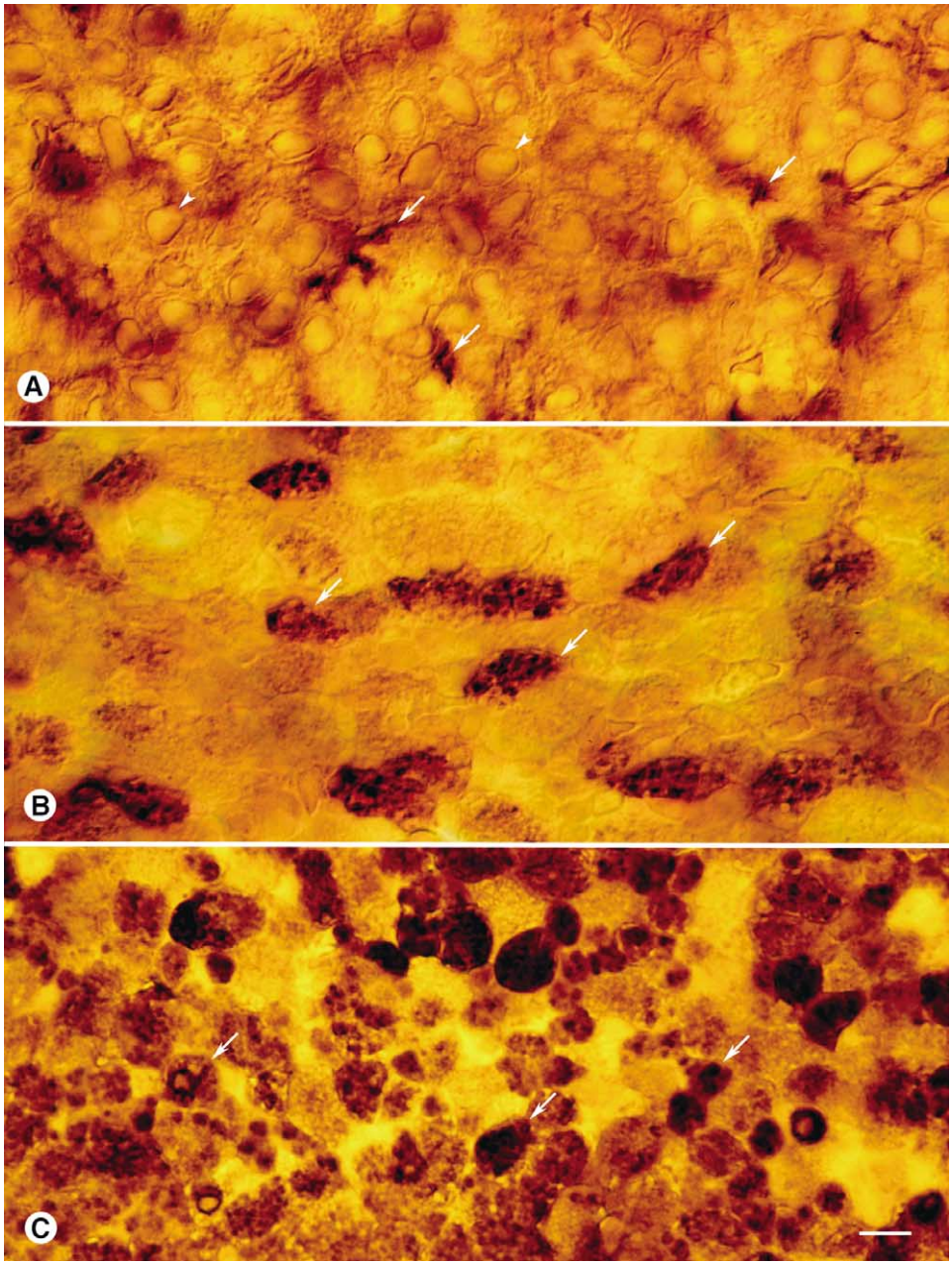

Fig. 4. Tracheal epithelial cells viewed from luminal surface of whole mounts. Comparison of OX6 immunoreactivity in tracheal epithelium of (A) pathogen-free rat, (B) *M. pulmonis*-infected rat at 2 days, and (C) *M. pulmonis*-infected rat at 1 week. Epithelial cells in pathogen-free rat (arrowheads) have little or no OX6 immunoreactivity, but some OX6-positive cells located beneath the epithelium have cytoplasmic processes (arrows) that extend into the epithelium. OX6-positive epithelial cells (arrows) are scattered in the epithelium of infected rat at 2 days. Many OX6-positive columnar epithelial cells (arrows) are present in infected rat at 1 week. Most of the immunoreactivity in these cells appears to be in intracellular granules. Scale bar in (C) applies to all figures. Bar = 8 μm (A–C).

4.1. Research strategy

Changes in the shape and number of OX6-positive cells were assessed after immunohistochemical staining of tracheal whole mounts. In these preparations, we could see the 3-dimensional shape as well as determine the distribution of cells in the mucosa. The 150-μm Vibratome sections complemented the whole mounts by highlighting the increase in mucosal thickness and the distribution of OX6-positive cells within the mucosa.

Only the most superficial OX6-positive cells were counted in whole mounts so the values could be related to data from previous studies [3]. Nonetheless, the number of these cells found in pathogen-free rats was 50–100% larger than corresponding values obtained from tangential 10 μm sections of mucosa just beneath

the epithelium [3]. This difference could be explained by the greater thickness of the region analyzed in the present study.

The combination of whole mounts and cross-sections produced a picture of OX6-positive cells that neither method could give independently and could not be readily obtained from conventional histological sections. Tracheal whole mounts provided a clear view of the number and 3-dimensional structure of OX6-positive cells in pathogen-free rats and during the first week after *M. pulmonis* infection. However, as the mucosa became thicker, only the most superficial cells of whole mounts were stained, probably due to limited penetration of reagents and increasing immunoreactivity of the epithelium. By comparison, cross-sections, which did not have the limitation of reagent penetration, clearly revealed the thickening of the mucosa and showed abundant OX6-positive cells throughout the mucosa. Together, the two types of preparations revealed that the total number of OX6-positive cells increased 6-fold over the first week after infection and 16-fold over 4 weeks.

4.2. Identification of OX6-immunoreactive cells

Pathogen-free animals. Most OX6-immunoreactive cells in the airways of pathogen-free rats are considered to be DC because they express MHC class II (Ia) determinants and have the characteristic dendriform morphology [3,4,27]. Holt and co-workers [4] reported that virtually all of the cells that stain for MHC class II in the airways of pathogen-free rats are DC. In addition, OX6-positive cells, which are most abundant at the base of the epithelium, can be distinguished from ED2-positive tissue macrophages, which are most numerous deeper in the mucosa [18]. Although tissue macrophages in pathogen-free rats may have cytoplasmic processes, they typically do not express MHC class II determinants in the absence of antigenic stimulation [29].

M. pulmonis-infected animals. The phenotypic distinction between DC and other cell types blurs after mycoplasmal infection, when multiple cell types express MHC class II molecules [30,31]. The characteristic branched morphology of DC in pathogen-free rats was no longer present in the OX6-positive cell population 1 week after infection and could, therefore, not be used to distinguish DC from other MHC class II expressing cells. Accordingly, some OX6-positive cells observed after infection may represent activated macrophages or B lymphocytes that have infiltrated the airway mucosa [15,31]. The exact proportion of DC relative to other MHC class II expressing cells cannot be definitively determined without using multiple cell markers. For example, activated B-cells could be identified by using OX12 as a marker [8]. However, it is unlikely that activated macrophages make a major contribution to the OX6-positive cell population, because in infected animals they acquire a distinctive distribution around angiogenic blood vessels, quite different from the pattern of OX6 immunoreactivity [18].

4.3. Changes in OX6-immunoreactive cell shape and number

In rats exposed to heat-killed *M. catarrhalis*, "small, round, intensely class II positive cells" migrate to the airway epithelium and reach a maximal density of approximately three times normal [32]. In sections of airway epithelium stained for OX6 immunoreactivity, class II-positive cells become pleomorphic about 8 h after challenge with *M. catarrhalis* and by 24 h develop into mature DC with highly branched processes [32]. Rounded DC precursors are not seen in control animals, and their transformation from rounded to stellate phenotype is most likely explained by local factors affecting DC maturation [5]. In our experiments, OX6-positive cells with a rounded phenotype accumulated in the airways during the first week after *M. pulmonis* infection. Perhaps the transformation from stellate to rounded phenotype reflects changes in DC maturation, differentiation, or motility. Alternatively, the apparent change in DC phenotype may represent the gradual replacement of stellate DC by rounded MHC class II expressing cells such as B-cells.

The number of OX6-positive cells remained fairly constant during the first 4 days after *M. pulmonis* infection and then increased significantly. The number continued to increase along with the 10-fold increase in thickness of the tracheal mucosa evident at 4 weeks. The accumulation of OX6-positive cells in the airway mucosa after *M. pulmonis* infection was accompanied by the accumulation of airway-associated lymphoid tissue [16,17].

Changes in the number of OX6-positive cells after intranasal inoculation of *M. pulmonis* differed both in onset and duration from what has been found after exposure to other bacteria or to viruses. Exposure to aerosolized bacteria can increase the number of OX6-positive DC within 1 h [5,6]. By contrast, the kinetics and time course of OX6-positive cell recruitment seen with *M. pulmonis* infection is closer to the response demonstrated by Sendai virus infection, which peaks at 3–5 days and remains elevated for 2 weeks [8]. Similarly, in rats exposed to heat-killed bacillus Calmette-Guérin, numerous OX6-positive DC accumulate at the borders of pulmonary granulomas, peaking at 2 weeks and then gradually decreasing [33].

4.4. Epithelial cells with OX6 immunoreactivity

The strong OX6 immunoreactivity of columnar epithelial cells that developed after *M. pulmonis* infection is consistent with the establishment of persistent infection

and the corresponding immune response. In pathogen-free rats, some basal cells had faint staining but other epithelial cells had none. After infection, immunoreactivity was detectable in scattered columnar epithelial cells at 2 days, was strong and fairly uniform at 1 week, and was still strong and uniform through 4 weeks. The upregulation of MHC class II determinants by airway epithelial cells has also been observed during Sendai virus infection [8]. Additionally, OX6 immunoreactivity has been reported in other types of epithelial cells after exposure to endotoxin or IFN-γ [9,10,34]. It is not clear whether the *M. pulmonis* organisms themselves or perhaps their ability to stimulate IFN-γ production is driving the MHC class II expression by epithelial cells. The granular immunoreactivity of epithelial cells resembles MHC-rich vacuoles in DC [35–37], where internalized antigen associates with MHC molecules.

4.5. Conclusions

M. pulmonis infection provides a potent immunologic stimulus that augments and transforms the MHC class II-expressing cell population of the airway mucosa. MHC class II-expressing cells become much more abundant in the mucosa during the first four weeks after infection, and concurrently, columnar epithelial cells begin to express MHC class II molecules. The rounding of OX6-positive cells after infection suggests that existing DC change shape during maturation or differentiation or are replaced by OX6-positive cells with a rounded phenotype. Changes in the OX6-positive cell population probably reflect the activation of an adaptive immune response and may play a role in the progression to chronic disease by persistently stimulating T lymphocyte responses.

Acknowledgments

The authors thank Dr. J. Russell Lindsey and Ms. Julie Erwin of the University of Alabama, Birmingham for supplying the *M. pulmonis* organisms and for helpful suggestions, Dr. Peter Baluk for assistance with the immunohistochemistry, Dr. Gary Anderson for insightful comments regarding the manuscript, and Dr. Gavin Thurston, Dr. John McLean, and Ms. Evelyn Clausnitzer for help throughout the project. This study was supported in part by NIH Grants HL24136 and HL59157 from the National Heart, Lung, and Blood Institute and Novartis Pharmaceuticals, Basel, Switzerland.

References

[1] R.M. Steinman, The dendritic cell system and its role in immunogenicity, Annu. Rev. Immunol. 9 (1991) 271–296.

[2] P.G. Holt, M.A. Schon-Hegrad, J. Oliver, MHC class II antigen-bearing dendritic cells in pulmonary tissues of the rat. Regulation of antigen presentation activity by endogenous macrophage populations, J. Exp. Med. 167 (1988) 262–274.

[3] M.A. Schon-Hegrad, J. Oliver, P.G. McMenamin, P.G. Holt, Studies on the density, distribution, and surface phenotype of intraepithelial class II major histocompatibility complex antigen (Ia)-bearing dendritic cells (DC) in the conducting airways, J. Exp. Med. 173 (1991) 1345–1356.

[4] P.G. Holt, M.A. Schon-Hegrad, J. Oliver, B.J. Holt, P.G. McMenamin, A contiguous network of dendritic antigen-presenting cells within the respiratory epithelium, Int. Arch. Allergy Appl. Immunol. 91 (1990) 155–159.

[5] A.S. McWilliam, D. Nelson, J.A. Thomas, P.G. Holt, Rapid dendritic cell recruitment is a hallmark of the acute inflammatory response at mucosal surfaces, J. Exp. Med. 179 (1994) 1331–1336.

[6] A.S. McWilliam, S. Napoli, A.M. Marsh, F.L. Pemper, D.J. Nelson, C.L. Pimm, P.A. Stumbles, T.N. Wells, P.G. Holt, Dendritic cells are recruited into the airway epithelium during the inflammatory response to a broad spectrum of stimuli, J. Exp. Med. 184 (1996) 2429–2432.

[7] P. Jecker, A. McWilliam, S. Napoli, P.G. Holt, R. Pabst, M. Westhofen, J. Westermann, Acute laryngitis in the rat induced by *Moraxella catarrhalis* and *Bordetella pertussis*: number of neutrophils, dendritic cells, and T and B lymphocytes accumulating during infection in the laryngeal mucosa strongly differs in adjacent locations, Pediatr. Res. 46 (1999) 760–766.

[8] A.S. McWilliam, A.M. Marsh, P.G. Holt, Inflammatory infiltration of the upper airway epithelium during Sendai virus infection: involvement of epithelial dendritic cells, J. Virol. 71 (1997) 226–236.

[9] M.K. Kim, A.G. Palestine, R.B. Nussenblatt, C.C. Chan, Expression of class II antigen in endotoxin induced uveitis, Curr. Eye Res. 5 (1986) 869–876.

[10] M. Platzer, D.S. Neufeld, L.A. Piccinini, T.F. Davies, Induction of rat thyroid cell MHC class II antigen by thyrotropin and γ-interferon, Endocrinology 121 (1987) 2087–2092.

[11] J.R. Lindsey, H.J. Baker, R.G. Overcash, G.H. Cassell, C.E. Hunt, Murine chronic respiratory disease. Significance as a research complication and experimental production with *Mycoplasma pulmonis*, Am. J. Pathol. 64 (1971) 675–708.

[12] G.H. Cassell, The pathogenic potential of mycoplasmas: *Mycoplasma pulmonis* as a model, Rev. Infect. Dis. 4 (1982) S18–S34.

[13] D.M. McDonald, T.R. Schoeb, J.R. Lindsey, *Mycoplasma pulmonis* infections cause long-lasting potentiation of neurogenic inflammation in the respiratory tract of the rat, J. Clin. Invest. 87 (1991) 787–799.

[14] H.T. Huang, A. Haskell, D.M. McDonald, Changes in epithelial secretory cells and potentiation of neurogenic inflammation in the trachea of rats with respiratory tract infections, Anat. Embryol. (Berl.) 180 (1989) 325–341.

[15] J.W. Simecka, S.E. Ross, G.H. Cassell, J.K. Davis, Interactions of mycoplasmas with B cells: antibody production and nonspecific effects, Clin. Infect. Dis. 17 Suppl 1 (1993) S176–S182.

[16] S. Watanabe, K. Watanabe, T. Ohishi, K. Kageyama, The development of extranodal lymphoid follicles in experimental bronchopneumonia, Acta Pathol. Jpn. 29 (1979) 533–543.

[17] G.J. van der Brugge-Gamelkoorn, M.B. van de Ende, T. Sminia, Non-lymphoid cells of bronchus-associated lymphoid tissue of the rat in situ and in suspension. With special reference to interdigitating and follicular dendritic cells, Cell Tissue Res. 239 (1985) 177–182.

[18] Å. Dahlqvist, E.Y. Umemoto, J.J. Brokaw, M. Dupuis, D.M. McDonald, Tissue macrophages associated with angiogenesis in chronic airway inflammation in rats, Am. J. Respir. Cell Mol. Biol. 20 (1999) 237–247.

[19] P. Baluk, J.J. Bowden, P.M. Lefevre, D.M. McDonald, Upregulation of substance P receptors in angiogenesis associated with chronic airway inflammation in rats, Am. J. Physiol. 273 (1997) L565–L571.
[20] T.R. Schoeb, K.C. Kervin, J.R. Lindsey, Exacerbation of murine respiratory mycoplasmosis in gnotobiotic F344/N rats by Sendai virus infection, Vet. Pathol. 22 (1985) 272–282.
[21] T.R. Schoeb, J.R. Lindsey, Exacerbation of murine respiratory mycoplasmosis by sialodacryoadenitis virus infection in gnotobiotic F344 rats, Vet. Pathol. 24 (1987) 392–399.
[22] J.J. Bowden, T.R. Schoeb, J.R. Lindsey, D.M. McDonald, Dexamethasone and oxytetracycline reverse the potentiation of neurogenic inflammation in airways of rats with *Mycoplasma pulmonis* infection, Am. J. Respir. Crit. Care Med. 150 (1994) 1391–1401.
[23] W.J. Xia, E.E. Schneeberger, K. McCarthy, R.L. Kradin, Accessory cells of the lung. II. Ia+ pulmonary dendritic cells display cell surface antigen heterogeneity, Am. J. Respir. Cell Mol. Biol. 5 (1991) 276–283.
[24] T.R. Schoeb, M.K. Davidson, J.R. Lindsey, Intracage ammonia promotes growth of *Mycoplasma pulmonis* in the respiratory tract of rats, Infect. Immun. 38 (1982) 212–217.
[25] M.K. Davidson, J.K. Davis, J.R. Lindsey, G.H. Cassell, Clearance of different strains of *Mycoplasma pulmonis* from the respiratory tract of C3H/HeN mice, Infect. Immun. 56 (1988) 2163–2168.
[26] P. Baluk, J. Nadel, D. McDonald, Calcitonin gene-related peptide is a marker of secretory cells of the rat tracheal epithelium, FASEB J. 5 (1992) A1268.
[27] J.J. Brokaw, G.W. White, P. Baluk, G.P. Anderson, E.Y. Umemoto, D.M. McDonald, Glucocorticoid-induced apoptosis of dendritic cells in the rat tracheal mucosa, Am. J. Respir. Cell Mol. Biol. 19 (1998) 598–605.
[28] D.M. McDonald, Endothelial gaps and permeability of venules in rat tracheas exposed to inflammatory stimuli, Am. J. Physiol. 266 (1994) L61–L83.
[29] P.G. Holt, J. Oliver, C. McMenamin, M.A. Schon-Hegrad, Studies on the surface phenotype and functions of dendritic cells in parenchymal lung tissue of the rat, Immunology 75 (1992) 582–587.
[30] Y. Naot, S. Merchav, E. Ben-David, H. Ginsburg, Mitogenic activity of *Mycoplasma pulmonis*. I. Stimulation of rat B and T lymphocytes, Immunology 36 (1979) 399–406.
[31] K. Yagyu, G. Steinhoff, H.J. Schafers, L. Dammenhayn, A. Haverich, H.G. Borst, Comparison of mononuclear cell subpopulations in bronchoalveolar lavage fluid in acute rejection after lung transplantation and Mycoplasma infection in rats, J. Heart Transplant. 9 (1990) 516–524.
[32] A.S. McWilliam, D.J. Nelson, P.G. Holt, The biology of airway dendritic cells, Immunol. Cell Biol. 73 (1995) 405–413.
[33] T. Tsuchiya, K. Chida, T. Suda, E.E. Schneeberger, H. Nakamura, Dendritic cell involvement in pulmonary granuloma formation elicited by bacillus Calmette-Guérin in rats, Am. J. Respir. Crit. Care Med. 165 (2002) 1640–1646.
[34] J. Lu, C. Kaur, E.A. Ling, Up-regulation of surface antigens on epiplexus cells in postnatal rats following intraperitoneal injections of lipopolysaccharide, Neuroscience 63 (1994) 1169–1178.
[35] R.M. Steinman, Z.A. Cohn, Identification of a novel cell type in peripheral lymphoid organs of mice. II. Functional properties in vitro, J. Exp. Med. 139 (1974) 380–397.
[36] R.M. Steinman, Z.A. Cohn, Identification of a novel cell type in peripheral lymphoid organs of mice. I. Morphology, quantitation, tissue distribution, J. Exp. Med. 137 (1973) 1142–1162.
[37] G. Schuler, N. Romani, R.M. Steinman, A comparison of murine epidermal Langerhans cells with spleen dendritic cells, J. Invest. Dermatol. 85 (1985) 99s–106s.

Since January 2020 Elsevier has created a COVID-19 resource centre with free information in English and Mandarin on the novel coronavirus COVID-19. The COVID-19 resource centre is hosted on Elsevier Connect, the company's public news and information website.